Highly Conductive Graphene Nanoribbons by Longitudinal Splitting of Carbon Nanotubes Using Potassium Vapor

Dmitry V. Kosynkin, Wei Lu, Alexander Sinitskii, Gorka Pera, Zhengzong Sun, and James M. Tour*

Richard E. Smalley Institute for Nanoscale Science and Technology, Department of Chemistry and Department of Mechanical Engineering and Materials Science, Rice University, 6100 Main Street, Houston, Texas, 77005, United States

ABSTRACT Here we demonstrate that graphene nanoribbons (GNRs) free of oxidized surfaces can be prepared in large batches and 100% yield by splitting multiwalled carbon nanotubes (MWCNTs) with potassium vapor. If desired, exfoliation is attainable in a subsequent step using chlorosulfonic acid. The low-defect density of these GNRs is indicated by their electrical conductivity, comparable to that of graphene derived from mechanically exfoliated graphite. The possible origins of directionally selective splitting of MWCNTs have been explored using computer modeling, and plausible explanations for the unique role of potassium were found.

KEYWORDS: graphene nanoribbons · potassium · chlorosulfonic acid · exfoliation

Graphene holds great promise for the fabrication of microelectronic devices. It is a zero-bandgap semiconductor demonstrating ballistic conductance over distances approaching several micrometers.[1−5] We have recently shown that multiwalled carbon nanotubes (MWCNTs) and single-walled carbon nanotubes (SWCNTs) can be selectively unzipped lengthwise by the action of acidic potassium permanganate to form straight-edged graphene oxide nanoribbons (GONRs).[6] Effectively using graphene can be hampered because the ballistic charge transport drops by several orders of magnitude if the sp^2 carbon network of ideal graphene is disrupted by even a relatively small number of defects.[7−11] The requisite low-defect material has only been available through treatments avoiding preliminary oxidation of graphite, including micromechanical cleavage,[1] chemical vapor deposition (CVD) on atomically flat surfaces of metal single crystals,[12,13] CVD on nickel[14] or copper foil,[15] or partial sublimation of silicon from the silicon face of SiC single crystals in high vacuum.[16] Splitting CNTs can directly produce graphene nanoribbons (GNRs) with high length-to-width ratios and dimensions exactly predetermined by the initial CNT length and diameter.[6] GNRs narrower than 10 nm have nonzero bandgaps inversely dependent upon their widths and are suitable for fabrication of low-voltage field effect transistors with up to 10^7 on/off ratios,[2] while the wider ribbons exhibit high electrical conductance characteristic of large graphene flakes and could be useful for bulk applications, such as flexible transparent electrodes. The high aspect ratio of wide GNRs might make them particularly attractive for carbon fiber spinning[17] and formulation of conductive polymer composites.[18]

To date, MWCNTs and SWCNTs have been unzipped to nanoribbons by treatment with permanganate in concentrated sulfuric acid.[6] Additionally, GNRs have been obtained by the cutting action of catalytic metal nanoparticle to give low yields of GNRs consisting of 50−100 layers,[19] by treatment of MWCNTs with a solution of lithium in liquid ammonia[20] and by plasma etching of polymer masked nanotubes.[21] The permanganate treatment, being a scalable process, produces heavily oxidized GONRs similar in chemical structure to graphene oxide (GO). While the majority of oxygen-containing functional groups can be removed from the basal plane of the GO ribbons by reduction, a small but significant fraction of defects persists even after annealing in hydrogen at 900 °C, resulting in lower electrical conductance dominated by a Mott variable range hopping mechanism instead of the desirable ballistic transport.[22] While oxidative defects are not introduced by the lithium/liquid ammonia intercalation-driven opening,[20] the process fails with pristine nanotubes; a preliminary treatment of the MWCNTs with a strong oxidant is required to induce defects that permit intercalation of

*Address correspondence to tour@rice.edu.

Received for review September 7, 2010 and accepted December 16, 2010.

Published online January 04, 2011
10.1021/nn102326c

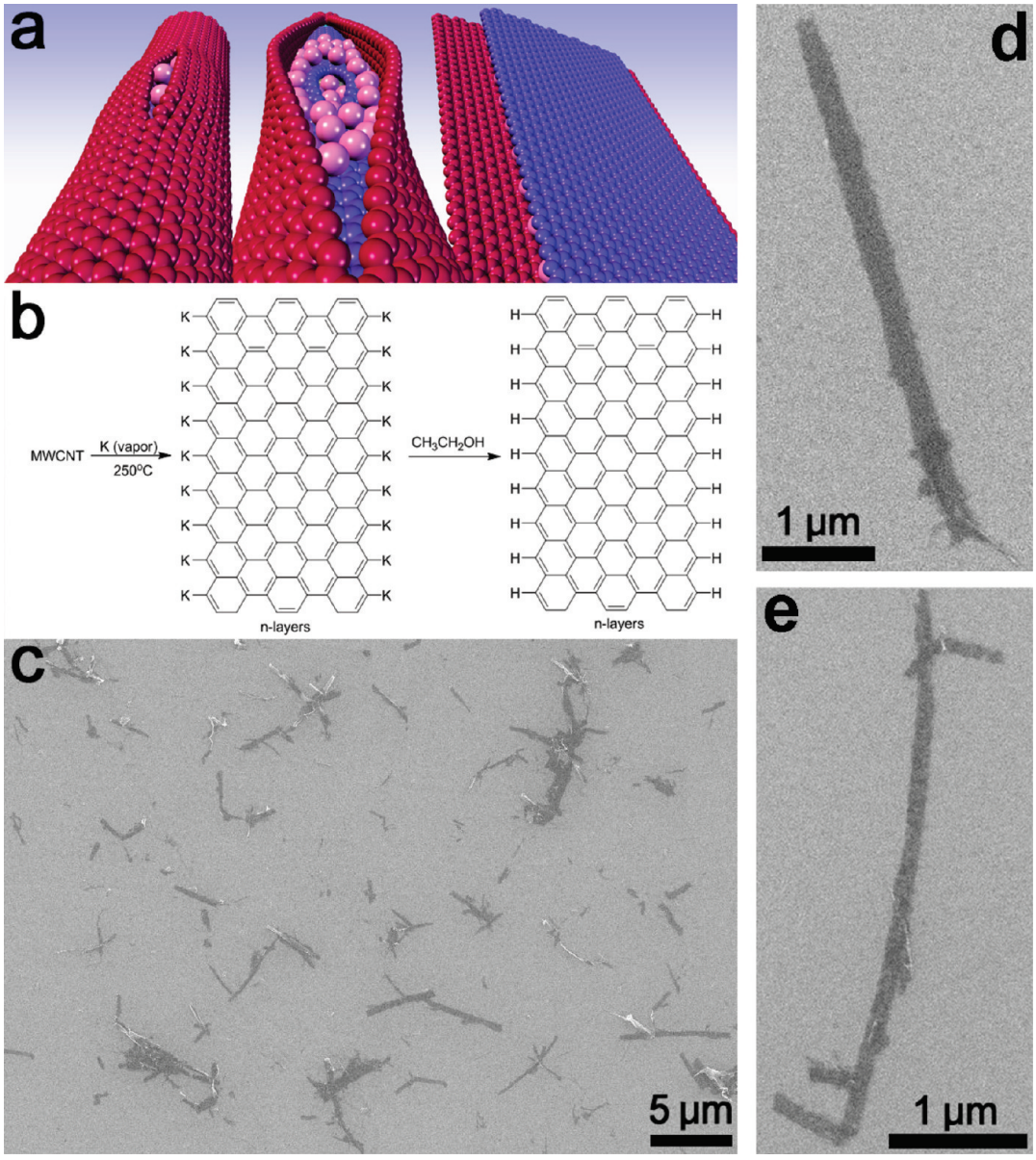

Figure 1. Schematic of the splitting process and SEM images on a Si/SiO_2 surface of GNRs produced by potassium splitting. (a) Schematic of potassium intercalation between the nanotube walls and sequential longitudinal splitting of the walls followed by unraveling to a nanoribbon stack. The potassium atoms along the periphery of the ribbons are excluded for clarity; see Figures S6−S9, Supporting Information for more details. (b) Chemical schematic of the splitting processes where ethanol is used to quench the aryl potassium edges; only a single layer is shown for clarity, while the actual number of GNR layers correlates with the number of concentric tubes in the MWCNT. (c) Overview of a large area showing complete conversion of MWCNTs to GNRs. (d, e), Images of isolated GNR stacks demonstrating characteristic high aspect ratios and predominantly parallel edges.

the ammonia-solvated lithium rendering defective ribbons that only partially unwrap from the tubular state.

Here, we investigate a hypothesis that thermal motion of a carbon framework in MWCNT sidewalls at elevated temperatures might create large enough transient openings for the alkali metal atoms to penetrate. In this process, potassium and MWCNTs, with a starting outside diameter of 40−80 nm and approximately 15−20 inner nanotube layers,[6] are sealed in a glass tube, heated in a furnace at 250 °C for 14 h, and followed by quenching with ethanol to effect the longitudinal splitting process in 100% yield, as depicted in Figure 1a and b. Intromission of potassium atoms results in the formation of intercalation compounds within the interstices of MWCNT sidewalls as commonly observed with other forms of graphitic carbon;[23,24] however, in the case of the MWCNTs used here, the splitting could be further assisted by the generation of H_2 upon the ethanolic quench.[25] Under sonication in chlorosulfonic acid, the split MWCNTs are further exfoliated to form GNRs. The use of high-quality pristine carbon nanotubes as GNR precursors allows production of material free from oxidative damage

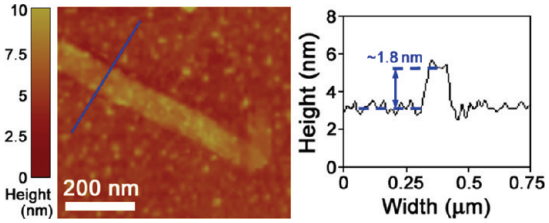

Figure 2. AFM image of a thin GNR with an average thickness of ~1.8 nm. The left panel shows a GNR with a folded end (lower-right portion), and the right panel shows the height of the ribbon along the blue line in the left panel. The GNR is likely a trilayer.

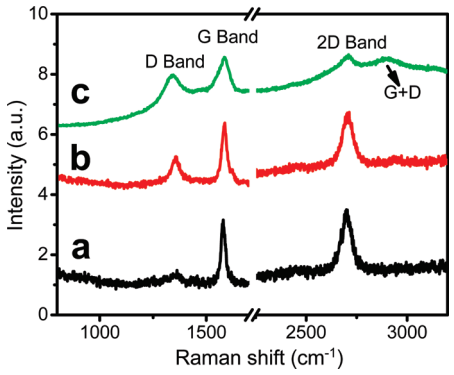

Figure 3. Raman spectra (excitation at 514 nm) of starting MWCNTs and splitting products. (a) Pristine MWCNTs. (b) MWCNTs treated with potassium at 250 °C generating split nanotroughs. (c) GNRs obtained after bath sonication of the material in (b) with chlorosulfonic acid for 24 h.

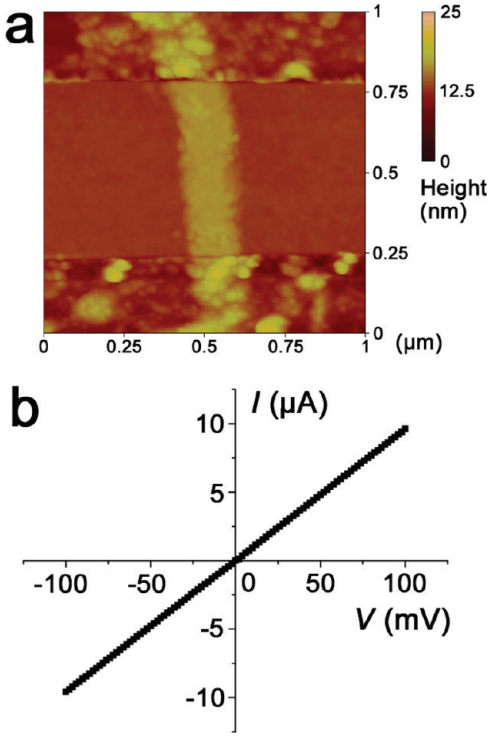

Figure 4. Appearance and electrical properties of a device made from a thin (3.8 nm) GNR stack. (a) AFM image of a GNR (~5-layered) with 0.5 μm-spaced platinum electrodes shown spanning horizontally at top and bottom. (b) Electrical properties (conductivity 80 000 S/m) of the GNR shown in (a).

and with conductivities paralleling the properties of the best samples of mechanically exfoliated graphene (measured on SiO_2 substrates). This simple, scalable, and inexpensive technique provides multigram quantities of stacked GNRs that can be further exfoliated with the aid of acid and mild bath sonication.

Scanning electron microscopy (SEM) and atomic force microscopy (AFM) were used to image the ribbon structures. SEM images in Figure 1 show the GNRs with widths of 130−250 nm and a length of 1−5 μm. AFM imaging (Figure 2) shows a thin graphene ribbon derived from the longitudinal splitting process. These results clearly indicate that MWCNTs were successfully split and then exfoliated to form GNRs after potassium intercalation followed by bath sonication in chlorosulfonic acid.

There was an increase in the ratio of intensities of Raman bands located around 1350 (D band) and 1580 cm^{-1} (G band) in comparison with the starting material (Figure 3). The D/G ratio[26] is commonly used as a measure of imperfection in the graphene lattice, as it corresponds to the relative population of sp^3-hybridized carbon atoms and it is also indicative of the abundance of edge atoms in the otherwise pristine flakes of mechanically exfoliated graphite.[1] The disordered structure introduced during the splitting and exfoliation process leads to the broadening of the G band[26,27] and the 2D band[28] as well as the combination mode[29] D + G band at about 2906 cm^{-1}.

To investigate the electrical properties of the GNRs derived from split tubes, several electronic devices were built on Si−SiO_2 and tested. The GNRs used for the device fabrication were 3.5−5 nm thick. All devices exhibited large conductivities ranging from ~70 000 to ~95 000 S/m, values that are comparable to other reported nanoribbons devices prepared from exfoliated graphene,[2,21] as seen in Figure 4. However, they showed only little gate effect, presumably due to the large number of layers in these GNRs and their high metal-like conductivity.

X-ray photoelectron spectroscopy (XPS) was also performed to determine whether the increase in the intensity of D band was caused by oxidation. No signals corresponding to C−O and C═O groups were observed in the high-resolution XPS C1s spectra (see Figures S3 and S4, Supporting Information). Thus, we conclude that the observed increase in the D/G ratio was solely attributable to the emergent edge carbon atoms and not an oxidative process. These MWCNT reductively derived GNRs are unlike chemically converted graphene (CCG) that is prepared by the reduction of GO. That latter protocol produces domains of graphene that are divided by defect boundaries, even upon extensive removal of oxygenation, resulting in their inferior electrical transport properties.[4]

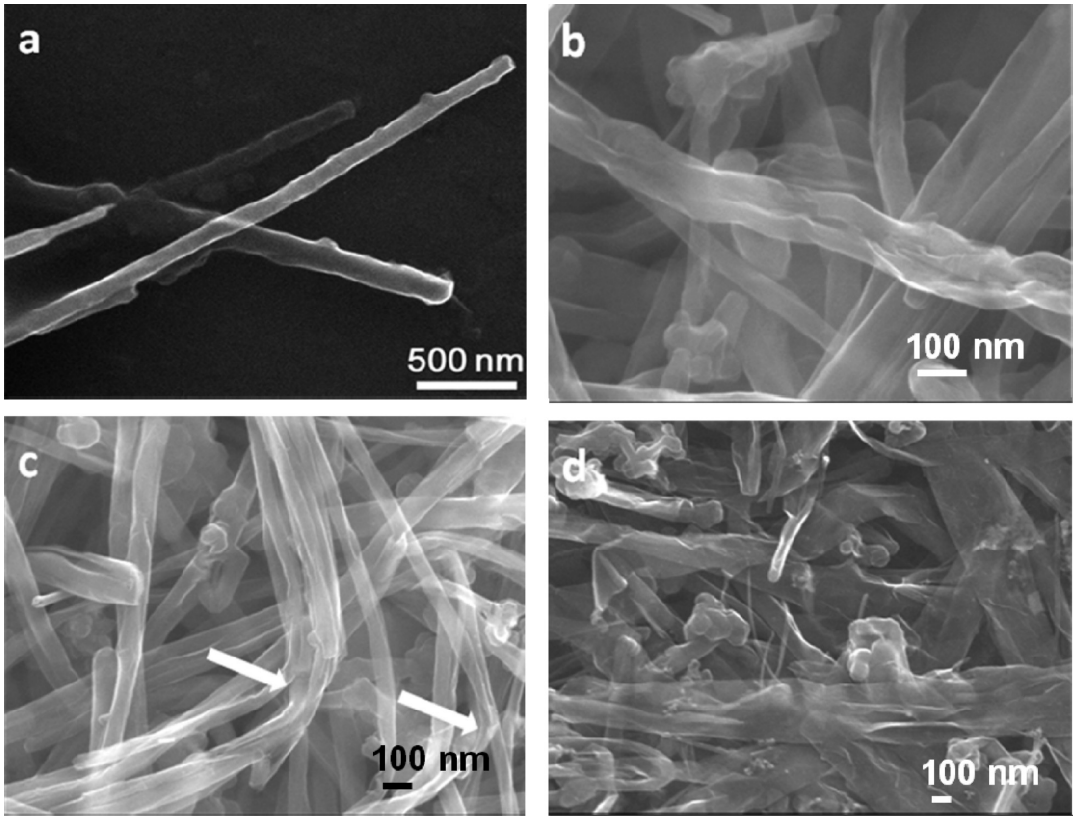

Figure 5. SEM images of MWCNTs treated with sodium and potassium. (a) MWCNTs recovered after treatment with sodium at 250 °C for 14 h showing no splitting. (b and c) MWCNTs treated with K at 250 °C for 14 h demonstrating a "split-log" appearance. Arrows indicate areas of high flexibility not observed in pristine MWCNT samples. (d) Potassium-treated MWCNTs after bath ultrasonication in chlorosulfonic acid for 24 h. Nearly complete conversion to stacks of straight-edged nanoribbons is evident.

Before we discuss the possible mechanism for splitting MWCNTs to form GNRs, let us briefly recall here the earlier experimental results on intercalation of alkali metals in graphite and carbon nanotubes. Graphite has a well-known propensity to form layered, stage I intercalation compounds when exposed to all molten alkali metals, except sodium, at moderately elevated temperatures. Intercalation of sodium proceeds anomalously as it requires using another metal, such as potassium, as a cointercalant or an application of high pressure (~2000 bar)[23] at which unusual double layers of intercalated metal can develop.[30] While the interaction of both MWCNTs and SWCNTs with alkali metals have been previously studied, no phenomena other than penetration of metal atoms into the spaces between individual nanotubes in nanotube bundles have been observed,[31,32] except by Cano-Márquez *et al.*,[20] where partial splitting of oxidatively cut MWCNTs arose after treatment with lithium dissolved in liquid ammonia, followed by quenching and thermal shocking. Unfortunately, when they intercalate alone, without a solvating shell of ammonia molecules, lithium atoms expand the interplanar distance in graphite from 0.335 nm to only 0.373 nm in C_6Li, the saturated stage I intercalation compound.[23] Such a small increase in the interstitial distance between the two outermost shells of a MWCNT would not likely provide enough strain in the carbon−carbon bonds to induce breakage at moderately elevated temperatures, and experimentally no splitting with lithium was observed.

Thus, we investigated the next larger metal, sodium. Although it is known that sodium does not well-intercalate into graphite,[23] we had to prove experimentally that MWCNTs were also poor targets for sodium intercalation. When MWCNTs were exposed to molten sodium and its vapor at 150−400 °C, no changes in sample appearance, nanotube morphology, or spectroscopic properties were observed. A representative SEM image of MWCNTs treated with sodium at 250 °C is shown in Figure 5a. Bond incommensurability is not thought to be an issue here because the MWCNTs interact not with solid sodium but with either molten or vaporized metal where those bonds are already broken.

Contrary to the results with lithium and sodium, the change in the nanotube behavior was dramatic when potassium was used (Figure 5b−d). The silvery luster of potassium rapidly changed at 150 °C to a uniform appearance of shiny golden-bronze color, as is seen for C_8K.[23] To obtain efficient intercalation, the reaction tube was heated for 14 h at temperatures varying from

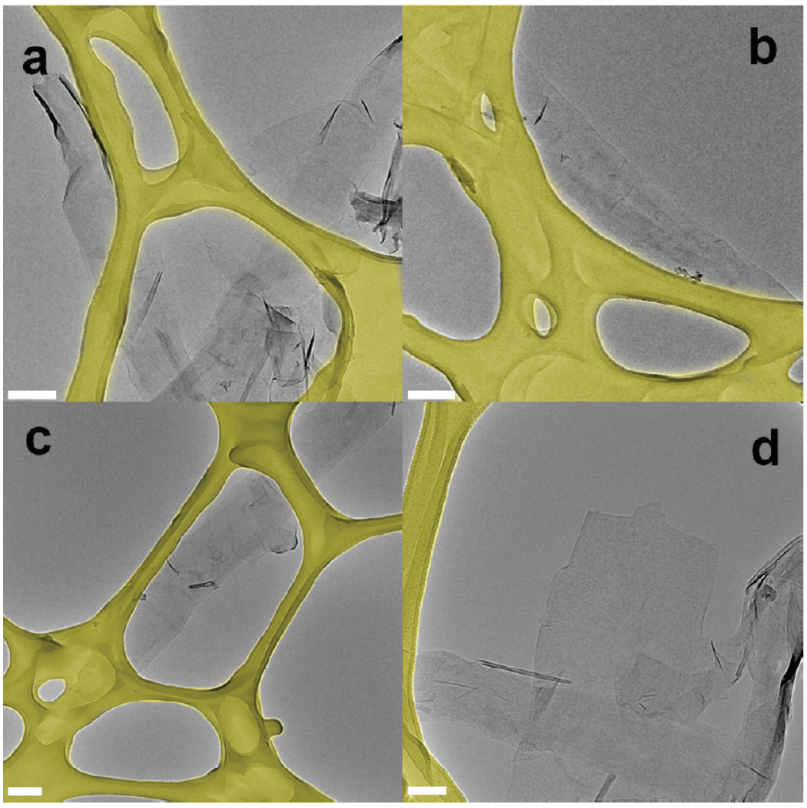

Figure 6. TEM images of GNRs obtained after sonication in chlorosulfonic acid for 24 h. (a−c) Few-layer GNRs. (d) Monolayer graphene nanoribbon. All scale bars are 200 nm, except for that in (d) (100 nm). The lacey carbon grid in the images is highlighted in yellow to make the GNRs more distinguishable. Complete exfoliation of MWCNTs to form GNRs is evident.

150 to 350 °C, and the 250 °C temperature was chosen for preparative purposes as the MWCNT splitting was complete at this temperature, while the Pyrex glass tube was not substantially corroded. The recovered product had much higher apparent density than the starting material, likely due to greater flexibility of the GNRs in comparison with the high-persistence length pristine MWCNTs. The enhanced suppleness of the nanotubes, resulting in bending and looping, was evident in the SEM images along with a "split-log" nanotrough appearance of individual MWCNTs (Figure 5 b and c). Formation of such curled nanotrough structures might be attributed to the incomplete splitting of MWCNTs. However, more likely, flattening of the resulting nanotrough is slow under the conditions employed due to the robust C−C bonds at the curled areas and the interlayer van der Waals interactions that would need to be overcome as the layers slide past each other upon flattening. Furthermore, fast deintercalation of the metal, as previously observed in the corresponding compounds of graphite,[25] could limit the entry of ethanol into the interstitial space. And since the initial study was performed in order to eliminate the exposure of the MWCNTs or subsequent GNRs to any oxidizing media, other means of exfoliation were sought.

After trying many organic solvents such as 1,2-dichlorobenzene and dimethylformamide, which did not induce the flattening and exfoliation, we chose chlorosulfonic acid as it has been shown to promote efficient exfoliation of bulk graphite to few-layer graphene; a superacid, such as chlorosulfonic acid, could protonate the split sidewalls of MWCNTs and thus induce electrostatic repulsive forces, which would facilitate exfoliation of split MWCNTs under sonication.[33] Therefore, we used a bath sonicator for 24 h to induce exfoliation in chlorosulfonic acid. Figure 5d shows the nanoribbons formed from exfoliation of split MWCNTs in chlorosulfonic acid under bath sonication. The advantage of bath sonication in the presence of a superacid was that electrostatic repulsive forces on the edges of split MWCNTs could overcome the van der Waals forces between the graphene layers, resulting in exfoliated GNRs. In order to distinguish the number of layers of GNRs, we carefully characterized the obtained sample using transmission electron microscopy (TEM). The TEM images in Figure 6 reveal that few-layered GNRs were obtained in the present case (see Supporting Information for high-resolution TEM images).

To further interpret the splitting of MWCNTs by potassium vapor, we used molecular dynamics to model the intercalation reaction. The simulation generates a MWCNT with a 30-atom cluster of potassium atoms, one atom thick, inserted into the interstitial void immediately beneath its outermost sidewall (see Supporting Information). The propagation of a cleft in the

sidewall should begin in a carbon "blister" formed around the intercalated potassium and would be driven by the concentration of strain at the tips of the fissure, aided by Coulomb repulsion of negative charges congregated at its edges and additionally enhanced by the buttressing interaction of carbon–potassium bonds decorating the newly formed edges. As the cleft expands, the surface of the nanotube wall one level closer to the core becomes exposed to potassium and, therefore, amenable to the intercalation-induced splitting.

Further simulation using rubidium and cesium with their larger ionic radii and lower ionization potentials shows that these metals should be even more effective at inducing MWCNT splitting than potassium. But the practical use of these metals is rather difficult owing to their pyrophoric nature and high costs. Interestingly, according to the simulation, SWCNTs should be immune to splitting by alkali metals, as their inner diameters, typically exceeding 0.7 nm, are large enough to accommodate any alkali metals without inducing additional strain in the sidewall of the tube. SWCNT splitting was not experimentally observed.

In conclusion, we have demonstrated a chemical route to produce bulk quantities of low-defect, highly conductive graphene nanoribbons and longitudinally split MWCNTs by exposing pristine nanotubes to hot potassium vapor followed by protonation. This was followed by bath sonication in chlorosulfonic acid to effect exfoliation of the highly stacked GNRs. Since the process does not require any oxidation, the less defective GNRs could result in intriguing electronic or spin properties. The GNRs could also be an attractive material for reinforcing polymers,[18] as the potassium-carrying reactive edges could facilitate the attachment of electrophiles or polymer chains to improve interfacial interaction for load transfer. Consequently, the present procedure opens up new directions for preparation of GNRs and subsequent applications.

EXPERIMENTAL SECTION

SEM imaging was performed on a JEOL-6500 field-emission microscope. AFM images were obtained with a Digital Instruments nanoscope IIIa, operating in tapping mode, using Si tips n-doped with 1–10 Ωcm phosphorus (Veeco, MPP-11100–140) at a scan rate of 0.5 Hz and a resolution of 512 × 512. XPS was performed on a PHI Quantera SXM scanning X-ray microprobe. Raman spectroscopy was performed on a Renishaw Raman microscope using a 633 nm HeNe laser. Fabrication of graphene devices was performed by tracking individual GNRs on the surface of highly doped Si substrates, covered with 500 nm-thick thermal SiO_2 layer, by SEM (JEOL-6500 microscope), and followed by patterning of 20 nm-thick Pt contacts by standard electron beam lithography, as described previously in detail.[22] The electrical transport properties were tested using a probe station (Desert Cryogenics TT-probe 6 system) under vacuum with chamber base pressure below 10^{-5} Torr. The IV data were collected by an Agilent 4155C semiconductor parameter analyzer.

Reaction of MWCNTs with Potassium. MWCNTs were provided by Mitsui & Co. (lot no. 05072001K28) and were used without any further treatment. The synthesis of potassium split MWCNTs was performed by melting potassium over MWCNTs under vacuum (0.05 Torr) as follows: MWCNTs (1.00 g) and potassium pieces (3.00 g) were placed in a 50 mL Pyrex ampule that was evacuated and sealed with a torch. (Caution: Potassium and sealing of the potassium-loaded ampule should be handled with utmost care due to the highly reactive nature of potassium metal. Users should wear safety glasses and a face shield, and all operations should be done in a sash-equipped fume hood when handling this reagent. Likewise, final quenching of potassium and its derivatives should be done with the utmost of care under an inert atmosphere.) The reaction mixture was kept in a furnace at 250 °C for 14 h. (Pyrex glass turns dark-brown when exposed to potassium vapor at 350 °C. This color disappears upon quenching with ethanol, but the glass surface shows visible signs of corrosion. Higher temperatures were not explored for safety reasons). The heated ampule containing a golden-bronze colored potassium intercalation compound and silvery droplets of unreacted metal was cooled to room temperature, opened in a drybox or in a nitrogen-filled glovebag, and then mixed with ethyl ether (20 mL). Ethanol (20 mL) was slowly added into the mixture of ethyl ether and potassium-intercalated MWCNTs at room temperature with some bubbling observed; much of the heat release was dissipated by the released gas (hydrogen). The quenched product was removed from the nitrogen enclosure and collected on a polytetrafluoroethylene (PTFE) membrane (0.45 μm), washed with ethanol (20 mL), water (20 mL), ethanol (10 mL), ether (30 mL), and dried in vacuum to give longitudinally split MWCNTs as a black, fibrillar powder (1.00 g).

Exfoliation of Potassium Split MWCNTs with Chlorosulfonic Acid. The potassium split MWCNTs tubes (10 mg) were dispersed in chlorosulfonic acid (15 mL, Sigma-Aldrich) under bath sonication using an ultrasonic jewelry cleaner (Cole-Parmer, EW-08849–00) for 24 h. (Caution: Chlorosulfonic acid must be handled with care since it is a corrosive liquid and reacts violently with water to form HCl and H_2SO_4. Users should wear protective gloves, a rubber smock, safety goggles, and a full-face shield, and all experiments should be performed in a sash-equipped and acid-approved fume hood.) The mixture was quenched by pouring onto ice (50 mL), and the suspension was filtered through a PTFE membrane (0.45 μm). The filter cake was dried under vacuum. The resulting black powder was dispersed in dimethylformamide (DMF) and bath sonicated for 15 min to prepare a stock solution for microscopy analysis.

Supporting Information Available: Additional XPS and UV–vis analytical spectra and TEM and SEM images of GNRs. Details of simulations of splitting and exfoliation of MWNTs. This material is available free of charge *via* the Internet at http://pubs.acs.org.

Acknowledgment. Mitsui & Co., Ltd. generously donated the MWCNTs. The work was funded by AFOSR (FA9550-09-1-0581), the AFOSR through University Technology Corporation (09-S568-064-01-C1), the Office of Naval Research Graphene MURI Program (00006766), and M-I SWACO, LLC. Gorka Pera gratefully acknowledges the award of a Formacion Profesorado Universitario fellowship from Ministerio de Educacion y Ciencia.

REFERENCES AND NOTES

1. Novoselov, K. S.; Geim, A. K.; Morozov, S. V.; Jiang, D.; Zhang, Y.; Dubonos, S. V.; Grigorieva, I. V.; Firsov, A. A. Electric Field Effect in Atomically Thin Carbon Films. *Science* **2004,** *306*, 666–669.

2. Li, X.; Wang, X.; Zhang, L.; Lee, S.; Dai, H. Chemically Derived, Ultrasmooth Graphene Nanoribbon Semiconductors. *Science* **2008,** *319*, 1229–1232.
3. Yang, L.; Park, C. H.; Son, Y. W.; Cohen, M. L.; Louie, S. G. Quasiparticle Energies and Band Gaps in Graphene Nanoribbons. *Phys. Rev. Lett.* **2007,** *99*, 186801–186804.
4. Gómez-Navarro, C.; Meyer, J. C.; Sundaram, R. S.; Chuvilin, A.; Kurasch, S.; Burghard, M.; Kern, K.; Kaiser, U. Atomic Structure of Reduced Rraphene Oxide. *Nano Lett.* **2010,** *10*, 1144–1148.
5. Novoselov, K. S.; Geim, A. K.; Morozov, S. V.; Jiang, D.; Katsnelson, M. I.; Grigorieva, I. V.; Dubonos, S. V.; Firsov, A. A. Two-Dimensional Gas of Massless Dirac Fermions in Graphene. *Nature* **2005,** *438*, 197–200.
6. Kosynkin, D. V.; Higginbothan, A. L.; Sinitskii, A.; Lomeda, J. R.; Dimiev, A. Longitudinal Unzipping of Carbon Nanotubes to Form Graphene Nanoribbons. *Nature* **2009,** *458*, 872–876.
7. Lusk, M. T.; Carr, L. D. D. Nanoengineering Defect Structures on Graphene. *Phys. Rev. Lett.* **2009,** *100*, 175503.
8. Chen, H. J.; Cullen, W. G.; Jang, C.; Fuhrer, M. S.; Williams, E. D. Defect Scattering in Graphene. *Phys. Rev. Lett.* **2009,** *102*, 236805.
9. Campos-Delgado, J.; Kim, Y. A.; Hayashi, T.; Morelos-Gómez, A.; Hofmann, M. P; Muramatsu, H.; Endo, M.; Terrones, H.; Shull, R. D.; Dresselhaus, M. S.; et al. Thermal Stability Studies of CVD-Grown Graphene Nanoribbons: Defect Annealing and Loop Formation. *Chem. Phys. Lett.* **2009,** *469*, 177–182.
10. Coleman, V. A.; Knut, R.; Grennberg, H.; Jansson, U.; Quinlan, R.; Holloway, B. C.; Sanyal, B.; Eriksson, O. Defect Formation in Graphene Nanosheets by Acid Treatment: an X-ray Absorption Spectroscopy and Density Functional Theory Study. *J Phys. D: Appl. Phys.* **2008,** *41*, 062001.
11. Hashimoto, A.; Suenaga, K.; Gloter, A.; Urita, K.; Iijima, S. Direct Evidence for Atomic Defects in Graphene Layers. *Nature* **2004,** *430*, 870–873.
12. Eizenberg, M.; Blakely, J. M. Carbon Monolayer Phase Condensation on Ni(111). *Surf. Sci.* **1979,** *82*, 228–236.
13. Aizawa, T.; Souda, R.; Otani, S.; Ishizawa, Y. Anomalous Bond of Monolayer Graphite on Transition-Metal Carbide Surfaces. *Phys. Rev. Lett.* **1989,** *64*, 768–771.
14. Kim, K. S.; Zhao, Y.; Jang, H.; Lee, S. Y.; Kim, J. M.; Kim, K. S.; Ahn, J.-H.; Kim, P.; Choi, J.-Y.; Hong, B. H. Large-Scale Pattern Growth of Graphene Films for Stretchable Transparent Electrodes. *Nature* **2009,** *457*, 706–710.
15. Li, X.; Cai, W.; An, J.; Kim, S.; Nah, J.; Yang, D.; Piner, R.; Velamakanni, A.; Jung, I.; Tutuc, E.; et al. Large-Area Synthesis of High-Quality and Uniform Graphene Films on Copper Foils. *Science* **2009,** *324*, 1312–1314.
16. Berger, C.; Song, Z.; Li, X.; Wu, X.; Brown, N.; Naud, C.; Mayou, D.; Li, T.; Hass, J.; Marchenkov, A. N.; et al. Electronic Confinement and Coherence in Patterned Epitaxial Graphene. *Science* **2006,** *312*, 1191–1196.
17. Ericson, L. M.; Fan, H.; Peng, H.; Davis, V. A.; Zhou, W.; Sulpizio, J.; Wang, Y.; Booker, R.; Vavro, J.; Guthy, C.; et al. Macroscopic, Neat, Single-Walled Carbon Nanotube Fibers. *Science* **2004,** *305*, 1447–1450.
18. Stankovich, S.; Dikin, D. A.; Dommett, G. H. B.; Kohlhaas, K. M.; Zimney, E. J.; Stach, E. A.; Piner, R. D.; Nguyen, S. T.; Ruoff, R. S. Graphene-Based Composite Materials. *Nature* **2006,** *442*, 282–286.
19. Elías, A. L.; Botello-Méndez, A. R.; Menese-Rodríguez, D.; González, V. J.; Ramírez-González, D.; Ci, L.; Muñoz-Sandoval, E.; Ajayan, P. M.; Terrones, H.; Terrones, M. Longitudinal Cutting of Pure and Doped Carbon Nanotubes to Form Graphitic Nanoribbons Using Metal Clusters as Nanoscalpels. *Nano Lett.* **2010,** *10*, 366–372.
20. Cano-Márquez, A. G.; Rodríguez-Macías, F. J.; Campos-Delgado, J.; Espinosa-González, C. G.; Tristán-López, F.; Ramírez-González, D.; Cullen, D. A.; Smith, D. J.; Terrones, M.; Vega-Cantú, Y. I. Ex-MWNTs: Graphene Sheets and Ribbons Produced by Lithium Intercalation and Exfoliation of Carbon Nanotubes. *Nano Lett.* **2009,** *9*, 1527–1533.
21. Jiao, L.; Zhang, L.; Wang, X.; Diankov, G.; Dai, H. Narrow Graphene Nanoribbons from Carbon Nanotubes. *Nature* **2009,** *458*, 877–880.
22. Sinitskii, A.; Fursina, A. A.; Kosynkin, D. V.; Higginbotham, A. L.; Natelson, D.; Tour, J. M. Electronic Transport in Monolayer Graphene Nanoribbons Produced by Chemical Unzipping of Carbon Nanotubes. *Appl. Phys. Lett.* **2009,** *95*, 253108.
23. Novikov, Y. N.; Vol'pin, M. E. Lamellar Compounds of Graphite with Alkali Metals. *Russ. Chem. Rev.* **1971,** *40*, 733–746.
24. Valles, C.; Drummond, C.; Saadaoui, H.; Furado, C. A.; He, M.; Roubeau, O.; Ortolani, L.; Monthioux, M.; Pénicaud, A. Solutions of Negatively Charged Graphene Sheets and Ribbons. *J. Am. Chem. Soc.* **2008,** *47*, 15802–15804.
25. Viculis, L. M.; Mack, J. J.; Kaner, R. B. A Chemical Route to Carbon Nanoscrolls. *Science* **2003,** *299*, 1361.
26. Ferrari, A. C.; Robertson, J. Interpretation of Raman spectra of disordered and amorphous carbon. *Phys. Rev. B: Condens. Matter Mater. Phys.* **2000,** *61*, 14095–14107.
27. Kudin, K. N.; Ozbas, B.; Schniepp, H. C.; Prud'homme, R. K.; Aksay, I. A.; Car, R. Raman Spectra of Graphite Oxide and Functionalized Graphene Sheets. *Nano Lett.* **2008,** *8*, 36–41.
28. Vidano, R.; Fischbach, D. B. New Lines in the Raman Spectra of Carbons and Graphite. *J. Am. Ceram. Soc.* **1978,** *61*, 13–17.
29. Campos-Delgado, J.; Romo-Herrera, J. M.; Jia, X.; Cullen, D. A.; Muramatsu, H.; Kim, Y. A.; Hayashi, T.; Ren, Z.; Smith, D. J.; Okuno, Y.; et al. Bulk Production of a New Form of sp^2 Carbon: Crystalline Graphene Nanoribbons. *Nano Lett.* **2008,** *8*, 2773–2778.
30. Suzuki, S.; Maeda, F.; Watanabe, Y.; Ogino, T. Electronic Structure of Single-Walled Carbon Nanotubes Encapsulating Potassium. *Phys. Rev. B: Condens. Matter Mater. Phys.* **2003,** *67*, 115418.
31. Duclaux, L.; Salvetat, J. P.; Lauginie, P.; Cacciaguera, T.; Faugère, A. M.; Goze-Bac, C.; Bernier, P. Synthesis and Characterization of SWNT-Heavy Alkali Metal Intercalation Compounds, Effect of Host SWNTs Materials. *J. Phys. Chem. Solids* **2003,** *64*, 571–581.
32. Guerard, D.; Herold, A. Intercalation of Lithium into Graphite and Other Carbons. *Carbon* **1975,** *13*, 337–345.
33. Behabtu, N.; Lomeda, J. R.; Green, M. J.; Higginbotham, A. L.; Sinitskii, A.; Kosynkin, D. V.; Tsentalovich, D.; Parra-Vasquez, A. N. G.; Schmidt, J.; Kesselman, E.; et al. Graphene Dispersion at High Concentrations and Formation of Liquid Crystals in Chlorosulfonic Acid. *Nat. Nanotech.* **2010,** *5*, 406–411.